Loss Minimization Design Using Magnetic Equivalent Circuit for a Permanent Magnet Synchronous Motor

Daisuke Sato
Department of Electrical Engineering
Nagaoka University of Technology
Nagaoka, Niigata, Japan
dsato@stn.nagaokaut.ac.jp

Jun-ichi Itoh
Department of Electrical Engineering
Nagaoka University of Technology
Nagaoka, Niigata, Japan
itoh@vos.nagaokaut.ac.jp

***Abstract*— This paper proposes a simple magnetic equivalent circuit using permeance method in order to design rough configurations of the lowest loss motor. First, the iron loss is calculated by the proposed method and compared with the analysis result by finite element method (FEM). As a result, the error of the calculation results between the proposed method and the FEM is 2.9%. Next, the motor losses are calculated by the proposed method when the several specifications are changed. As a result, these results agree in principle with that of the FEM. Therefore, the validity of the proposed method is confirmed. In addition, the method of the motor design is considered in terms of the loss.**

Keywords*— Permanent magnet synchronous motor, Loss minimization design, Permeance method, Finite element method

I. INTRODUCTION

Recently, the permanent magnet synchronous motor (PMSM) is actively researched in order to achieve the high efficiency in the motor drive system. In addition, the PMSM is not only high efficiency but also smaller than the induction motor. Therefore, the PMSM is applied to the electric vehicle and the home electric appliance [1-4].

The analysis of the loss, the torque and the back electromotive force are important in terms of further improvement of the motor. Generally, the characteristics of the motor are analyzed by the finite element method (FEM) [5-7]. However, the FEM spends much analysis time. Moreover, the development of the motor model is required as often as modifying the configuration of the motor. Hence, the FEM is not suitable for the calculation of the optimized solution such as the maximum torque density or the lowest loss point because much time of trial and error is needed to find the optimization point.

On the other hand, the permeance method is used in order to design the motor simply in the past. In the permeance method, a magnetic circuit is replaced with an electric circuit. In this method, the magnetic flux and the magnetomotive force can be expressed as the current and the voltage. Therefore, this method is suitable for the optimized solution because of shorter calculation time, although the calculation accuracy of the permeance method is less than that of the FEM. This is because the magnetic circuit of the motor is primarily determined as the distributed constant circuit.

The permeance network method has been proposed as one of the motor characteristic analysis using the permeance method [8-11]. This method expresses the stator, the rotor and the air gap on a magnetic circuit. The torque and the back electromotive force can be calculated by calculating the magnetic flux in the air gap from the magnetic circuit. However, the magnetic resistance of the air gap depends on a position of the magnetic pole. Therefore, the construction of the magnetic circuit is complex. On the other hand, the method, which calculates eddy current loss in the permanent magnet, has been proposed [12]. In this method, the eddy current loss can be accurately calculated in comparison with the FEM. However, the calculation process is complicated. In addition, the equation is changed when the shape of the motor is changed.

Generally, first, rough configurations such as size, pole number, teeth width are decided in the design of IPMSM. After that, the details such as flux barrier are decided. Therefore, it is considered that the simple loss calculation is enough in the phase of rough design.

In this paper, the simple magnetic equivalent circuit using permeance method is proposed in order to design the rough configurations of the lowest loss motor. The characteristic of the equivalent circuit is separation between rotor and stator. Therefore, the complex calculations are not needed because the magnetic resistance of air gap can become constant. In addition, if the shape of motor is changed, the magnetic resistance and the magnetomotive force are changed only. Thus, the circuit is not changed.

First, this paper presents the calculation method of flux density in stator core. Next, the loss of IPMSM is calculated and the result is compared with the analysis result of FEM and the measurement result. Finally, the lowest loss motor is designed by the loss calculation in the changing parameter of IPMSM

II. MAGNETIC EQUIVALENT CIRCUIT OF PMSM

Generally, in the permeance method, the magnetic circuit is replaced with an equivalent electric direct current circuit. However, it takes the time variation of the magnetic flux density to calculate the iron loss. Therefore, the conventional permeance method is not applied directly. In addition, it is difficult to express as one circuit because the rotor is rolling and the stator is not rolling. Therefore, the magnetic flux in the air gap is calculated by the equivalent circuit of the rotor. Next, the time variation of the magnetic flux density in the teeth and yoke are calculated by the equivalent circuit of the stator. It is noted that the input of the stator circuit is the magnetic flux in the air gap.

Fig. 1 shows the model of the IPMSM and Table I shows the parameters of the IPMSM. The motor is the concentrated winding IPMSM. In addition, the permanent magnets are magnetized in parallel and mounted in the motor. Furthermore, the motor has periodicity every 60 degrees.

Fig. 2 shows the equivalent magnetic circuit of the rotor. It is noted that the equivalent circuit comprises of the half of one pole region. This is because the region of 30 degrees is able to be regarded as symmetry. The magnetic resistance R is given by (1).

$$R = \frac{l}{\mu S} \tag{1}$$

It is noted that μ is the magnetic permeability, S is the cross section of the material, and l is the length of the material. The magnetic resistance of the rotor core is not taken into consideration because it is sufficiently smaller than the magnetic resistance of the magnet. In addition, the magnetomotive force of the magnet F_m is expressed as

$$F_m = H_e l_m \tag{2}$$

where H_e is the coercive force of the magnet and l_m is the length of the magnet. Further, the magnetic saturation is expressed by the magnetic resistance R_{sat} which varies by the magnetomotive force because the magnetic saturation occurs in the area between the magnet and the outer of the rotor. Thus, the magnetic flux in the air gap is calculated.

Fig. 3 shows the equivalent magnetic circuit of the stator. This circuit comprises the magnetic resistance of the air gap, the teeth, the yoke and some magnetomotive forces. The magnetomotive force by the flowing current to the armature winding F_i is expressed as

$$F_i = NI_m \sin(\omega t + \theta) \tag{3}$$

where N is the number of winding turns per the teeth, $I_m\sin(\omega t+\theta)$ is the instantaneous current. In addition, the

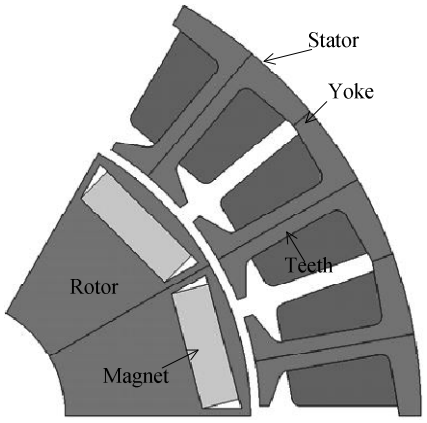

Fig. 1 Concentrated winding IPMSM. The magnets are magnetized in parallel. The motor has periodicity every 60 degrees.

TABLE I PARAMETERS OF IPMSM.

Core	35H300 / Nippon Steel
Magnet	NMX-41SH / Hitachi Steel
Number of poles	12
Number of slots	18
Coil turns per teeth	11
Outer diameter of stator	100 mm
Inner diameter of stator	66 mm
Outer diameter of rotor	64 mm
Inner diameter of rotor	25 mm
Air gap length	1 mm
Iron stack length	50 mm
Magnet dimensions	$12.5\text{mm}\times 25\text{mm}\times 4\text{mm}$

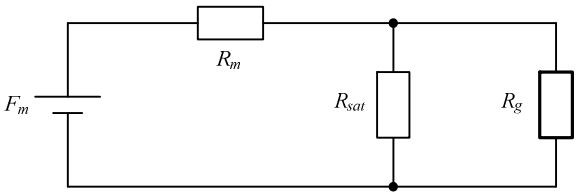

Fig. 2 Magnetic equivalent circuit of rotor. The circuit consists of the half of one pole region. In this circuit, the flux in air gap is calculated.

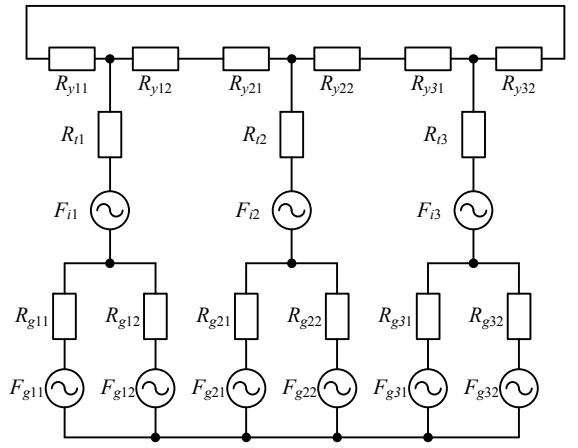

Fig. 3 Magnetic equivalent circuit of stator. The AC magnetomotive force F_g and F_i are set. The magnetic resistance is considered the magnetic saturation. In this circuit, the flux densities in teeth and yoke are calculated.

AC magnetomotive force F_g is set as the element

generated the magnetic flux in the air gap. As a result, the effect of the rolling rotor can be considered.

Fig. 4 shows the waveform of magnetomotive force F_g. it is assumed that F_g is trapezoidal waveform owing to the layout of the magnet. The waveform of F_g is determined from the proportion of the magnet width and the teeth width. The phase of the magnetomotive force ϕ_g is determined from the position of the teeth and expressed as

$$\phi_g = \frac{2\pi}{\theta_p}\theta_t \qquad (4)$$

where θ_t is the position of the teeth and θ_p is the angle of one period.

Further, it is necessary for the magnetic resistance of the teeth and the yoke to consider the magnetic saturation. Therefore, the magnetic resistance depends on the magnetomotive force in the magnetic saturation region. Accordingly, the time variation of the magnetic flux density in the teeth and the yoke are calculated. Moreover, the iron loss in the stator core can be calculated by the magnetic flux density of the teeth and the yoke.

III. Calculation of Magnetic Flux Density and Iron Loss

The magnetic flux density and the iron loss are calculated by the permeance method. Furthermore, the calculation results by applying the permeance method are compared with that of the FEM. Table II lists the calculation conditions of the permeance method. The armature current is sinusoidal waveform.

Fig. 5 shows the FEM model of the concentrated winding IPMSM. The magnetic flux density and the iron loss are analyzed by two-dimensional FEM using JMAG Designer (JSOL). It is noted that the number of elements is 6,525 and the time interval per 1 step is 2.71 μs (1024 steps).

Fig. 6 shows the waveform of the magnetic flux density calculated by the permeance method and the FEM. Accordingly, the waveform of the teeth by the permeance method is saturated at 1.75 T. Moreover, it is similar to the waveform of the teeth by the FEM. However, the peak of the magnetic flux density in the yoke by the permeance method is drastically changed. Therefore, the waveform of the yoke by the permeance method is different from the waveform by the FEM.

Fig. 7 shows the harmonic analysis result of the magnetic flux density. From Fig. 7, the fundamental component of the permeance method almost agrees with that of the FEM. However, the error occurs at the odd order harmonic component by the magnetomotive force. Especially, the 3rd order and 9th order components by the permeance method do not occur because the equivalent circuit of the stator is the balanced three-phase circuit. Next, the iron loss in the stator is calculated from the magnetic flux density and the iron loss curve of the material.

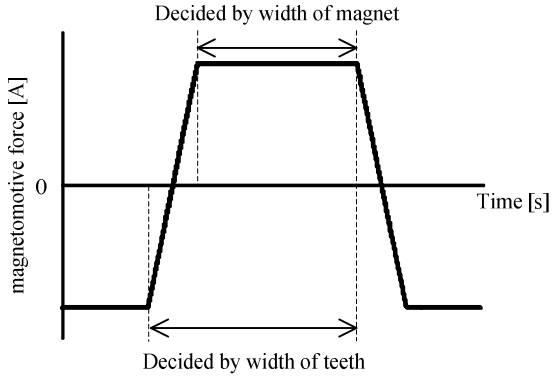

Fig. 4 Waveform of magnetomotive force. The waveform is determined from the proportion of the magnet width and the teeth width.

TABLE II Calculation Conditions.

Armature current		18 A_{rms}
Motor speed		3600 r/min
Electrical frequency		360 Hz
Magnetic resistance	Teeth	7.0×10^4 A/Wb
	Yoke	5.9×10^4 A/Wb
	Gap	3.4×10^6 A/Wb

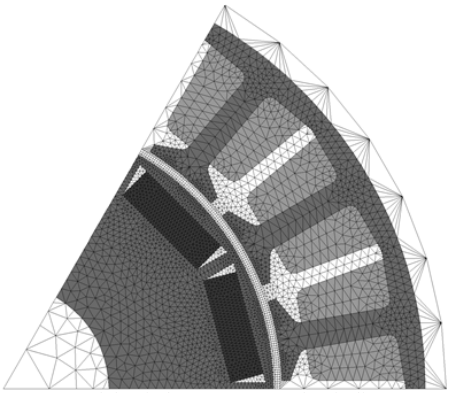

Fig. 5 FEM model of the concentrated winding IPMSM. The number of elements is 6,525. Time interval per 1 step is 2.71 μs (1024 steps).

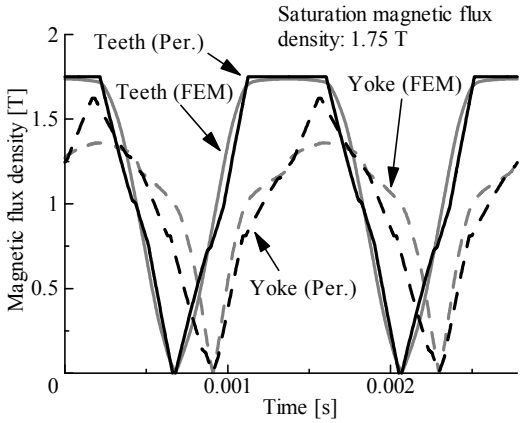

Fig. 6 Waveform of magnetic flux density by permeance method and FEM. The waveform of the teeth by the permeance method is similar to that by the FEM

Fig. 8 shows the iron loss curve of the material

(35H300 / Nippon Steel). As shown in Fig. 8, the iron losses at the required frequency are not shown. For this reason, the iron losses at the required frequency are calculated by the linear interpolation. As the result, it is confirmed that the iron loss in the stator is 30.4 W and the calculated iron loss by the FEM is 31.3 W. The error between the permeance method and the FEM is 2.9%.

IV. Comparison with Iron Loss Measurement Result

The motor loss is measured and compared with calculation result in order to confirm the validity of the loss calculation by the proposed method. The IPMSM is typically driven by the inverter. If the carrier frequency is low, the motor loss by harmonic component of the output voltage should be considered. However, the loss can be reduced by the high carrier frequency. In addition, the 3-level inverter can reduce not only the harmonic component of the output voltage but also the switching loss compared with the 2-level inverter. Therefore, in this paper, the motor loss by the carrier harmonics is ignored on the assumption that the IPMSM is driven by the 3-level inverter.

Fig. 9 shows the construction of IPMSM loss measurement system. The parameters of the test motor are shown Fig.1 and Table 1. The 3-level T-type neutral point clamped inverter is applied to IPMSM loss measurement system. In addition, the input power of the motor is measured by the power meter (WT1800/YOKOGAWA) and the shaft power is calculated based on the measurement result of the output torque by the torque meter (TH-2105/Ono sokki).

Fig. 10 shows the measurement result of the motor loss at 3600 r/min. The motor loss is reduced due to the increasing carrier frequency. The reason is that the harmonic component in the output voltage of the inverter is reduced. However, the motor loss is almost unchanged over 7520 Hz. Therefore, the output voltage is equivalent to sinusoidal voltage over 7520 Hz. In this section, the motor loss at 7520 Hz is compared with the calculation results of the proposed method and the FEM because the carrier frequency is ignored.

Next, the iron loss P_{Fe} is separated from the motor loss P_{loss}. The copper loss P_{Cu} and the mechanical loss P_m are expressed by (5) and (6), respectively. The mechanical loss is calculated by the empiric formula of windage loss because it is assumed that the friction loss of bearing is negligible small. Therefore, the iron loss is expressed by (7).

$$P_{Cu} = 3R_a I^2 \tag{5}$$

$$P_m = 8D(l + 0.15)v_a{}^2 \tag{6}$$

$$P_{Fe} = P_{loss} - P_{Cu} - P_m \tag{7}$$

where, R_a is wire resistance per one-phase, I is root mean square value of line current, D is outer diameter of rotor, l is length of rotor and v_a is peripheral speed of rotor.

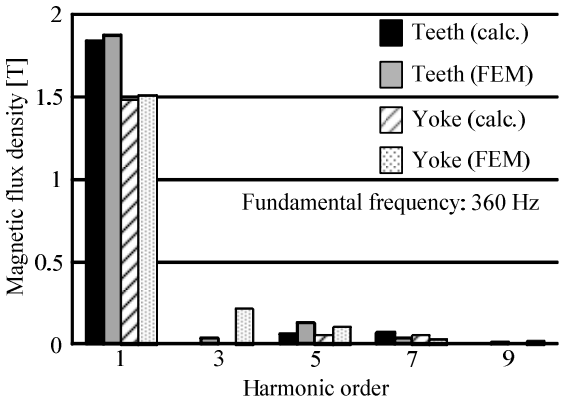

Fig. 7 Harmonic component of magnetic flux density. The fundamental component by applying the permeance method almost agrees with that of the FEM.

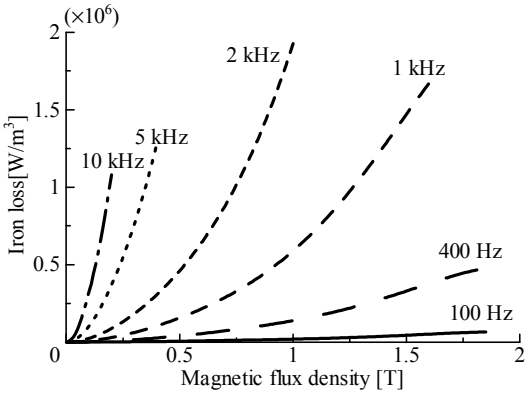

Fig. 8 Iron loss curve of 35H300 (Nippon Steel). The iron losses at the required frequency are calculated by the linear interpolation.

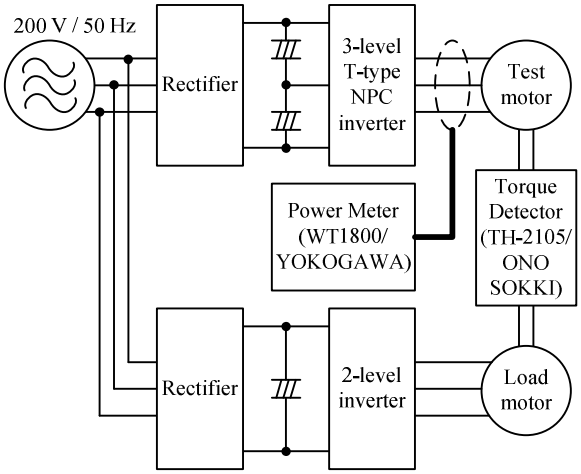

Fig. 9 IPMSM loss measurement system. The test motor is driven by the 3-level T-type neutral point clamped inverter. The input power of the motor is measured by the power meter. The shaft power is calculated based on the measurement result of the output torque.

Fig. 11 shows the measurement and calculation results of the iron loss at 3600 r/min and 2.3 Nm. The error between the calculation result by proposed method and the analysis result by FEM is caused by the loss in the rotor and the magnets. In addition, the error between the

analysis result and the measurement result is less than 1%. Therefore, it is assumed that the error is the stray load loss. Thus, the validity of the proposed method is confirmed.

V. MOTOR DESIGN OF LOWEST LOSS

The motor loss is calculated by the proposed method when the mechanical parameter is changed. Moreover, the lowest loss motor is designed based on the calculation results.

Fig. 12 shows the flowchart of the motor design of the lowest loss. 1) Topology of magnetic equivalent circuit is decided based on the configuration of IPMSM. 2) Specifications of the motor are decided. 3) Magnetic resistance and Magnetomotive force in the rotor circuit are calculated. 4) Flux in the air gap is calculated by the equivalent circuit of the rotor. 5) Magnetomotive force is set to the equivalent circuit of the stator from the flux in the air gap. 6) The flux density in stator core is calculated. 7) Iron loss of the stator core is calculated by the flux density and iron loss curve of the core. In addition, copper loss is calculated by the wire resistance and the line current. 8) After, the losses are calculated in several specifications, the lowest loss motor is selected. In this section, the cases of changing pole/slot number, lengths of axial/radial direction and length of teeth are considered.

A. Changing Pole and Slot Number

If the proposed magnetic equivalent circuit is applied to the model changing pole number, the frequency of the magnetomotive force has to be changed only. Therefore, the reconstitution of the circuit is not required. In this section, it is assumed that the ratio between pole number and slot number is constant.

Fig. 13 shows the analysis models of 8 poles 12 slots motor and 16 poles and 24 slots motor. The angles of one period are 90 and 45 degrees, respectively. In addition, the 12 poles 16 slots motor is also calculated and shown in Fig.1. The outer diameter of the rotor and the stator, the lengths of the air gap and the axial direction, the turn number of the coil and the volume of the magnets are constant. The area of slots is changed by the changing slot number. Therefore, the space factor of the coil is constant (50%) and the area of wire (i.e. the resistance of wire) is changed. Moreover, the speed is 3600 r/min. In terms of the output torque, the amplitude of current is adjusted so as to become 3.9 Nm in the FEM. In addition, the amplitude of current in the proposed method is decided by the flux in the air gap.

Fig. 14 shows the motor loss by the changing pole number and slot number based on the constant volume. The motor loss is standardized by the volume. Therefore, if it is assumed that the current density and the magnetic flux density are constant, the calculation result can also be applied to the motor of the different volume. The errors between the proposed method and the FEM are less than 10% in the all models. In addition, the trend of changing loss in the proposed method agrees with that in the FEM. Furthermore, in this case, the loss of 12 poles 16 slots motor is the lowest.

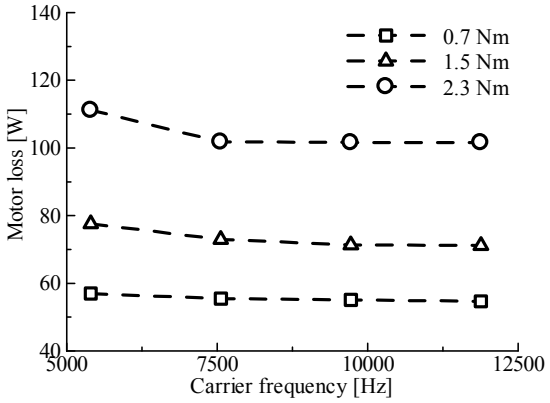

Fig. 10 Measurement result of IPMSM loss at 3600 r/min. The loss is almost unchanged over 7520 Hz because the harmonic component in the output voltage of the inverter is low.

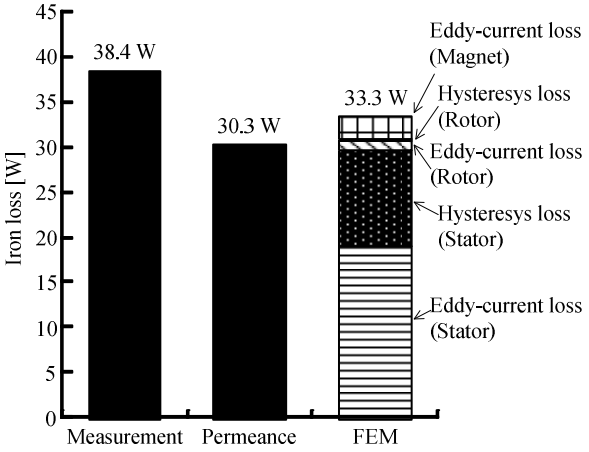

Fig. 11 Measurement result and calculation result by permeance method and FEM of iron loss (3600 r/min, 2.3 Nm). The error between the calculation result by proposed method and the analysis result by FEM is caused by the loss in the rotor and the magnets.

The loss of the 12 poles motor is smaller than that of the 8 poles motor. The reason is that the current can be become small under the same output torque by increasing pole number. However, the resistance of wire increases because the area of slot becomes small. Therefore, the loss of the 16 poles motor is larger than that of the 12 poles motor. In addition, the width of the teeth can become large by decreasing pole number and slot number. Therefore, the iron loss decreases by the decreasing flux density. On the other hand, if the pole number and slot number are increased, the iron loss increases because the stator core is saturated magnetically.

B. Changing Lengths of Axial and Radial Direction

Fig. 15 shows the schematic of the changing radial direction length and axial direction length. The calculation conditions are as follows; the motor shown in Fig. 2 is used. The volume of the motor is constant and the axial direction length D and the radius r are changed. The air gap length is set to 1 mm by adjusting the size of the rotor. The amplitude of the armature current is

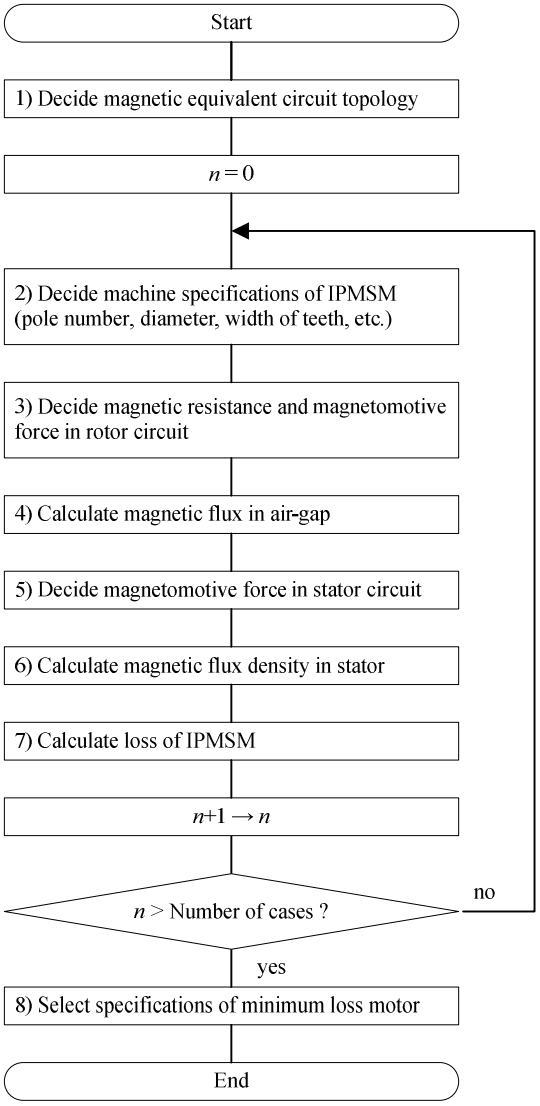

Fig. 12 Flowchart of the motor design of the lowest loss. The lowest loss motor can be designed by the calculating the losses in several specifications.

calibrated because the output torque is set to constant. The motor speed is 3600 r/min. The copper loss and the iron loss in the stator are calculated.

Fig. 16 shows the motor loss when the axial direction length and the radius are changed. The radius r is standardized by the axial direction length D and the loss is standardized by the volume of the motor. From the calculation result by the permeance method in Fig. 15, the motor loss decreases when the size is enlarged to the radial direction. In addition, the analysis results by the FEM agree in principle with that of the permeance method. Therefore, the validity of the loss calculation by using the permeance method is confirmed.

If the size is enlarged to the radial direction, the magnetic flux in the air gap decreases because the magnetic resistance of the air gap and the magnet increases. Therefore, the large current is required in order to keep the magnetic flux. However, the wiring resistance can be decreased because the cross section of the coil winding can be enlarged and the length of the coil

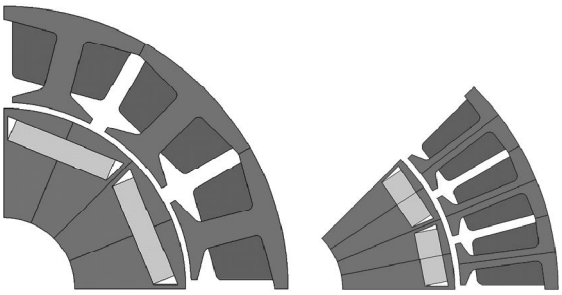

Fig. 13 IPMSM models of changing pole number. The angles of one period are 90 and 45 degrees, respectively. The outer diameter of the rotor and the stator, the lengths of the air gap and the axial direction, the turn number of the coil and the volume of the magnets are constant.

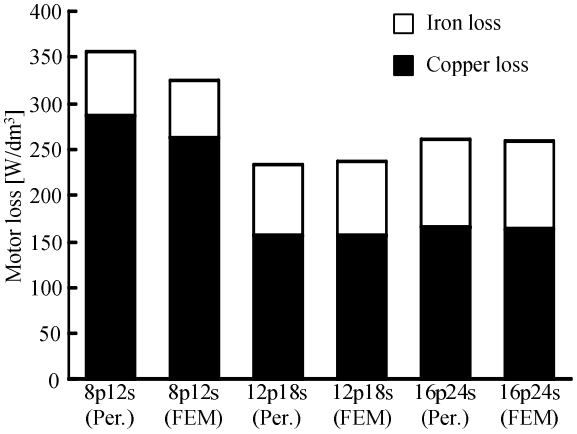

Fig. 14 Motor loss at 3600 r/min and 3.9 Nm by the changing pole number and slot number based on the constant volume. The loss is standardized by the volume. The errors between the proposed method and the FEM are less than 10% in the all models. The loss of 12 poles 16 slots motor is the lowest in this case.

winding can become short. Thus, the copper loss can be decreased. On the other hand, if the size is enlarged to the axial direction, the magnetic flux increases in order to decrease the magnetic resistance. However, the magnetic flux density decreases because the cross section of the stator core is enlarged at a great rate. Therefore, the iron loss can be decreased. For these reason, the copper loss and the iron loss are in the relationship of trade-off. As a result, the motor loss is decreased by enlarging to the radial direction because the variation of the copper loss is larger than that of the iron loss. If the current density becomes low, the variation of the iron loss has a significant impact on the motor loss and the lowest loss point exists.

C. Changing Length of Teeth Width

Fig. 17 shows the schematic of the changing teeth width. The losses are calculated when the width of the teeth is changed based on the constant width of the yoke. In addition, the area of the coil is changed by the changing teeth width. Therefore, the space factor of the coil is constant (50%) and the resistance of wire is changed. Moreover, the speed is 3600 r/min and the output torque is 3.9 Nm.

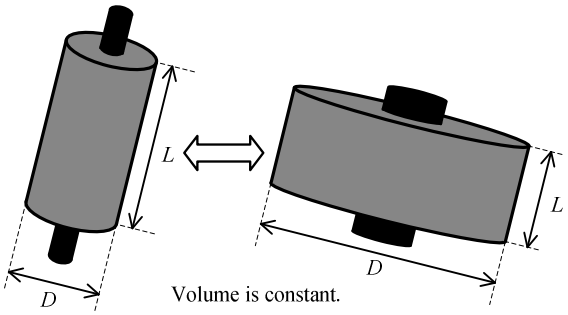

Fig. 15 Schematic of the changing radial direction length *D* and axial direction length *L* The air gap length is set to 1 mm by adjusting the size of the rotor. The amplitude of the armature current is calibrated because the output torque is set to constant. The motor speed is 3600 r/min. The copper loss and the iron loss in the stator are calculated..

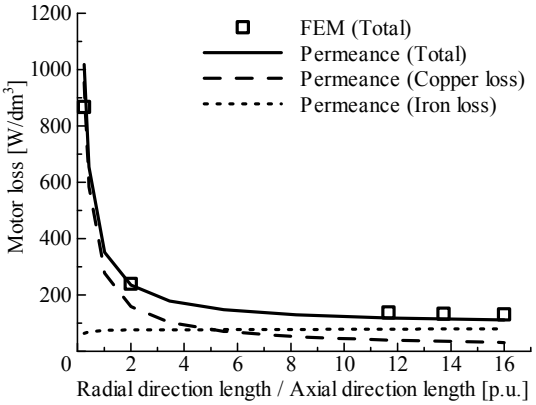

Fig. 16 Motor loss at 3600 r/min and 3.9 Nm when the radial direction length and the axial direction length are changed based on the constant volume. The radius *r* is standardized by the axial direction length *D* and the loss is standardized by the volume of the motor. The motor loss decreases when the size is enlarged to the radial direction.

Fig. 18 shows the motor loss when the teeth width is changed based on the constant volume. The teeth width is standardized by the yoke width and the loss is standardized by the volume of the motor. The trend of changing loss in the proposed method agrees with that in the FEM. In addition, when the teeth width is 1.8 p.u., the loss is the lowest in the calculation results by the proposed method. On the other hand, in the results by the FEM, when the width is 2.0 p.u., the loss is the lowest. The difference between the loss at 1.8 p.u. and 2.0 p.u. is very few. Thus, it is considered that the teeth width of minimum loss can be designed by the proposed method.

If the teeth width is become large, the magnetic resistance decreases and the flux in the core increases. Therefore, in less than 1.6 p.u., the iron loss increases due to the increasing flux density of yoke. However, in over 1.6 p.u., the iron loss decreases because the flux density of the teeth decreases. In addition, the flux in the air gap increases by the increasing flux in the core. If the output torque is same, the current can be decreased. Thus, the copper loss can be decreased. However, in over 1.8 p.u., the copper loss increases because the area of coil become small and the resistance of wire become large.

From these results, when the motor parameters are

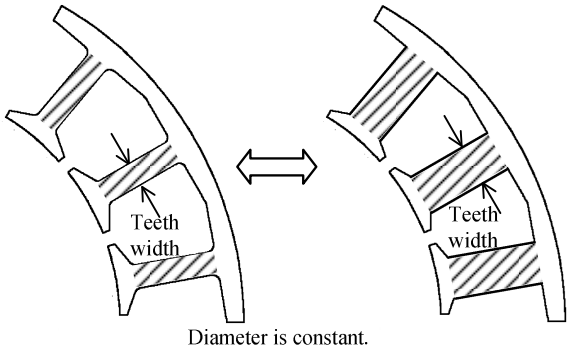

Fig. 17 Schematic of the changing teeth width. The yoke width is constant. The area of the coil is changed by the changing teeth width. The space factor of the coil is constant (50%) and the resistance of wire is changed

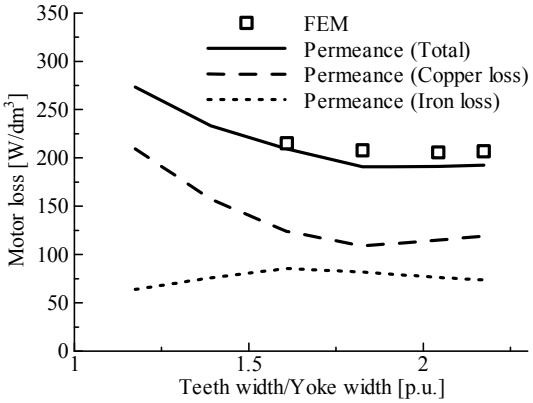

Fig. 18 Motor loss at 3600 r/min and 3.9 Nm when the teeth width is changed based on the constant volume. The loss at 1.8 p.u. is the lowest in the calculation results by the proposed method.

changed, it is confirmed, the validity of loss calculation by the proposed method. Therefore, the minimum loss motor can be designed. For example, if the mechanical strength is considered and the diameter is less than 2 p.u. as a constrained condition, the parameter of the minimum loss motor is as follows: the pole number is 12, the diameter is 2 p.u. and the teeth width is 1.8 p.u..

VI. CONCLUSIONS

This paper proposed the simple magnetic equivalent circuit in order to design the rough configurations of the lowest loss motor. As a result, the error of the iron loss between the proposed method and the FEM is 2.9%. In addition, the motor losses were calculated by the permeance method when several parameters were changed. As a result, these results are almost agreed in principle with the results of the FEM. Therefore the validity of the proposed method was confirmed.

The future works are as follow; first, the eddy current loss in the permanent magnet will be calculated by the permeance method. Second, the motor loss considered the carrier harmonics will be calculated.

REFERENCES

[1] G. Pellegrino, et al. “Performance Comparison Between Surface-Mounted and Interior/min Motor Drives for Electric Vehicle Application”, IEEE Trans. Ind. Electron., Vol.59, No.2, 2012.

[2] D. G. Dorrell, A. M. Knight, L. Evans, and M. Popescu, "Analysis and Design Techniques Applied to Hybrid Vehicle Drive Machines—Assessment of Alternative IPM and Induction Motor Topologies", IEEE Transactions on Industrial Electronics, Vol.59, No.10, pp.3690-3699 (2012)

[3] X. Yuan and J. Wang, "Torque Distribution Strategy for a Front- and Rear-Wheel-Driven Electric Vehicle", IEEE Transactions on Vehicular Technology, Vol.61, No.8, pp.3365-3374 (2012).

[4] R. Cao, C. Mi, and M. Cheng, "Quantitative Comparison of Flux-Switching Permanent-Magnet Motors With Interior Permanent Magnet Motor for EV, HEV, and PHEV Applications", IEEE Transactions on Magnetics, Vol.48, No.8, pp.2374-2384 (2012)

[5] T. Okitsu, D. Matsuhashi and K. Muramatsu, "Method for Evaluating the Eddy Current Loss of a Permanent Magnet in a PM Motor Driven by an Inverter Power Supply Using Coupled 2-D and 3-D Finite Element Analyses", IEEE Transactions on Magnetics, Vol.45, No.10, pp.4574-4577 (2009)

[6] K. Yamazaki and N. Fukushima, "Iron-Loss Modeling for Rotating Machines: Comparison Between Bertotti's Three-Term Expression and 3-D Eddy-Current Analysis", IEEE Transactions on Magnetics, Vol.46, No.8, pp.3121-3124 (2010)

[7] Y. Kawase, T. Yamaguchi, T. Umemura, Y. Shibayama, K. Hanaoka, S. Makishima, and K. Kishida, "Effects of carrier frequency of multilevel PWM inverter on electrical loss of interior permanent magnet motor", ICEMS 2009, LS5A-2 (2009)

[8] J. Farooq, S. Srair, A. Djerdir and A. Miraoui, "Use of Permeance Network Method in the Demagnetization Phenomenon Modeling in a Permanent Magnet Motor", IEEE Transactions on Magnetics, Vol.42, No.4, pp.1295-1298 (2006)

[9] B. Sheikh-Ghalavand, S. Vaez-Zadeh and A. H. Isfahani, "An Improved Magnetic Equivalent Circuit Model for Iron-Core Linear Permanent-Magnet Synchronous Motors", IEEE Transactions on Magnetics, Vol.46, No.1, pp.112-120 (2010)

[10] A. R. Tariq, C. E. Nino-Baron, and E. G. Strangas, "Iron and Magnet Losses and Torque Calculation of Interior Permanent Magnet Synchronous Machines Using Magnetic Equivalent Circuit", IEEE Transactions on Magnetics, Vol.46, No.12, pp.4073-4080 (2010)

[11] G. Gotovac, G. Lampic and D. Miljavec "Analytical Model of Permeance Variation Losses in Permanent Magnets of the Multipole Synchronous Machine", IEEE Transactions on Magnetics, Vol.49, No.2, pp.921-928 (2013)

[12] N. Leboeuf, T. Boileau, B. Nahid-Mobarakeh, N. Takorabet, F. Meibody-Tabar, and G. Clerc, "Inductance Calculations in Permanent-Magnet Motors Under Fault Conditions", IEEE Transactions on Magnetics, Vol.48, No.10, pp.2605-2616 (2012)